DOI 10.1515/epoly-2013-0001 — e-Polymers 2014; 14(1): 75–84

Ulises Páramo-Garcia, Angelica Avalos-Perez, Javier Guzman-Pantoja, Nancy Patricia Díaz-Zavala, Jose Aaron Melo-Banda, Nohra Violeta Gallardo-Rivas, Juan Reyes-Gómez, Dario Pozas-Zepeda, Jorge G. Ibanez and Nikola Batina*

Polypyrrole microcontainer structures and doughnuts designed by electrochemical oxidation: an electrochemical and scanning electron microscopy study

Abstract: Scanning electron microscopy (SEM) is employed to monitor the surface morphology of polypyrrole films (PPy) grown on different working electrodes (i.e., vitreous carbon and Au (111)) under diverse experimental conditions (i.e., dynamic vs. static potential protocols) and anion dopants (i.e., I^- and F^-). The morphology of the electrosynthesized films includes rings (doughnuts) and microcontainers, and depends on the synthesis parameters such as the electropolymerization method, the nature of the substrate, the anion dopant, and the sequence of sandwich composite growth. The formation of well-defined rings and microcontainers is attributed to overoxidation occurring during the formation of F^--doped PPy. It is possible to design microcontainers by controlling the overoxidation and degradation of the polymer surface.

Keywords: anionic dopant; conducting polymer; electrosynthesis; microcontainers; polypyrrole.

***Corresponding author: Nikola Batina,** Lab. de Nanotecnologia e Ing. Molecular, Area de Electroquimica, Depto. de Quimica, CBI, Universidad Autonoma Metropolitana-Iztapalapa, Av. San Rafael Atlixco 186, Col. Vicentina, 09340 Mexico, D.F., Mexico, e-mail: bani@xanum.uam.mx

Ulises Páramo-Garcia: Lab. de Nanotecnologia e Ing. Molecular, Area de Electroquimica, Depto. de Quimica, CBI, Universidad Autonoma Metropolitana-Iztapalapa, Av. San Rafael Atlixco 186, Col. Vicentina, 09340 Mexico, D.F., Mexico; and Division de Estudios de Posgrado e Investigacion, Instituto Tecnologico de Cd. Madero, Juventino Rosas y Jesus Urueta S/N, Col. Los Mangos, 89440 Cd. Madero, Tamps., Mexico

Angelica Avalos-Perez: Lab. de Nanotecnologia e Ing. Molecular, Area de Electroquimica, Depto. de Quimica, CBI, Universidad Autonoma Metropolitana-Iztapalapa, Av. San Rafael Atlixco 186, Col. Vicentina, 09340 Mexico, D.F., Mexico

Javier Guzman-Pantoja: Instituto Mexicano del Petroleo, Eje Central Lázaro Cardenas, Norte 152, Col. San Bartolo Atepehuacan, 07730 Mexico. D.F., Mexico

Nancy Patricia Díaz-Zavala, Jose Aaron Melo-Banda and Nohra Violeta Gallardo-Rivas: Division de Estudios de Posgrado e Investigacion, Instituto Tecnologico de Cd. Madero, Juventino Rosas y Jesus Urueta S/N, Col. Los Mangos, 89440 Cd. Madero, Tamps., Mexico

Juan Reyes-Gómez and Dario Pozas-Zepeda: Facultad de Ciencias, Universidad de Colima, Bernal Diaz del Castillo 340, Col. Villas San Sebastian, 28045 Colima, Col. Mexico

Jorge G. Ibanez: Centro Mexicano de Química Verde y Microescala. Dept. de Ing. y C. Quimicas, Universidad Iberoamericana, Prol. Reforma 880, 01219 México, D.F., Mexico

1 Introduction

Interest in conducting polymers has grown considerably because of their applications in microelectronic, electrochromic, biomedical devices, rechargeable batteries, anticorrosion films, chemical and biochemical sensors, protection against electromagnetic radiation, antistatic packaging, and the like (1–14). Modern developments of new custom-designed polymers that partially or completely replace classical materials increase their range of applications (15–17). This is especially true in the field of conductive polymers like polypyrrole, which can be produced both chemically and electrochemically (14, 18). Electrochemical polymerization leads to the formation of a polymer film on the surface of the working electrode. This offers several advantages including the controllability of thickness, morphology, and conductivity (14, 19). Since its seminal electrochemical preparation in 1968, polypyrrole (PPy) has been one of the most extensively used and studied conductive polymers (18, 20–22).

PPy has proven suitable as a candidate for the controlled release of substances because of its unique redox properties, which offer, for instance, the possibility of controlled drug administration through electrical stimulation (23, 24). Other applications are related to the analytical determination of drugs in biological samples (25), the fabrication of solid-state potentiometric sensors (26), and its use as an adsorbent in the solid-phase microextraction of organic compounds (27). Most of these applications stem from suitable electrical properties of the

polymer that have been studied, for example, by four-probe conductivity (28) and electrochemical impedance spectroscopy (29).

The formation of microcontainers in PPy films opens new possibilities to the use of new materials in the drug delivery arena. There are many methods available to modify polymer films based on physical and chemical pre- and/or post-treatments (30–35). The nature of the solvent and electrolyte used during the electrochemical synthesis of PPy largely determines its final properties (36). In the present study, we used two different doping anions in aqueous solution to synthesize conducting PPy films with dissimilar final morphologies, showing that the formation of microcontainers is related to the polymer film overoxidation.

2 Materials and methods

Electrochemical formation of PPy films was achieved by cyclic voltammetry and constant potential methods. A conventional three-electrode cell was used at room temperature (20±3°C). A vitreous carbon disk electrode (VC, Bioanalytical Systems, West Lafayette, Indiana, MF-2012, 0.07 cm^2) and a coated-glass Au (111) electrode (Arrandee, G.T., Werther, Germany, 0.075 cm^2) were used as working electrodes (WEs). The surface of the VC was polished using alumina powder (0.25 µm MicroDi, South Bay Technology, San Clemente, CA, USA and 0.10 µm, Allied High Tech Products, Rancho Dominguez, CA, USA), and then sonicated (Branson, Danbury, CT, USA 2510R-MT). Lastly, the electrode was rinsed with distilled water and ethanol (50/50 v/v) for 15 min and washed with acetone before using it in the electrochemical cell.

All the experiments were performed using a BAS potentiostat (Model 100B, Bioanalytical Systems). All potentials are referred to a $Ag/AgCl_{(sat)}$ electrode (BAS, MF-2052) separated from the medium by a Vycor membrane. A Pt mesh (0.6 cm^2, 99.99%) was used as the auxiliary (counter) electrode. The electrolytes were 0.1 mol/L aqueous solutions of KI and KF (J. T. Baker, reagent grade). A 0.1 mol/L pyrrole solution was prepared after distillation of reagent-grade pyrrole (Py, Aldrich, 98%) in a nitrogen atmosphere. All the solutions were prepared with Millipore water (18.2 MΩ) deaerated during 10–15 min with pure nitrogen (Praxair, 99.99%) before the experiments. Scanning electron microscopy (SEM, Peabody, MA, USA, JEOL-JSM-6390LV) with energy-dispersive spectroscopy (EDS; NCA x-Stream Module, Oxford Inst., Tubney Woods, Abingdon, Oxfordshire, UK) was used to observe the surface characteristics of the polymer films.

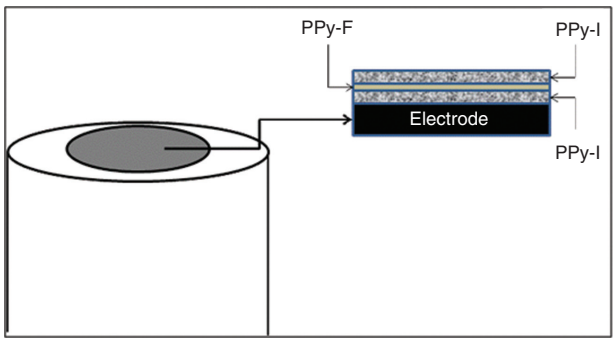

Figure 1 Schematic representation of the polymer sandwich composite formation.

To design polymer sandwich composites, I^- and F^- were used as dopant anions following the experimental configuration of Figure 1. The design varied according to the layer formation sequence: WE:PPy-I:PPy-F:PPy-I or WE:PPy-F:PPy-I:PPy-F.

3 Results and discussion

In order to explain the selection of two particular dopant anions (F^- and I^-), it is important to note some of their differences. F^- is a large hydrated anion, whereas I^- is very small and does not possess a hydrated shell. Previous studies show that the thickness and morphology of PPy films depend on several key parameters (37–39), one of which is the nature of the dopant ion (34). For the present case, the PPy layers formed electrochemically in the presence of I^- are much thicker and more conductive than those formed in the presence of F^- (40). Also, significant differences are observed in the resulting PPy film morphology as described below.

3.1 Electropolymerization of PPy films

Figure 2 shows cyclic voltammograms for PPy film growth in (A) 0.1 mol/L KI and (B) 0.1 mol/L KF solutions, using 10 polymerization cycles in a potential range from -0.5 to +0.9 V vs. Ag/AgCl at a scan rate v=100 mV/s.

The peaks observed between -0.40 and +0.50 V during polymerization in KI solution (Figure 2A) correspond to the charge and discharge of the PPy film (14, 41) accompanied by the reduction/oxidation of the I_2/I^- couple (42–44). The cathodic response indicates that an important amount of iodine species became trapped within the polymeric matrix. The electrochemical polymerization is indeed known to be catalyzed by the I_2/I^-couple [35]. The

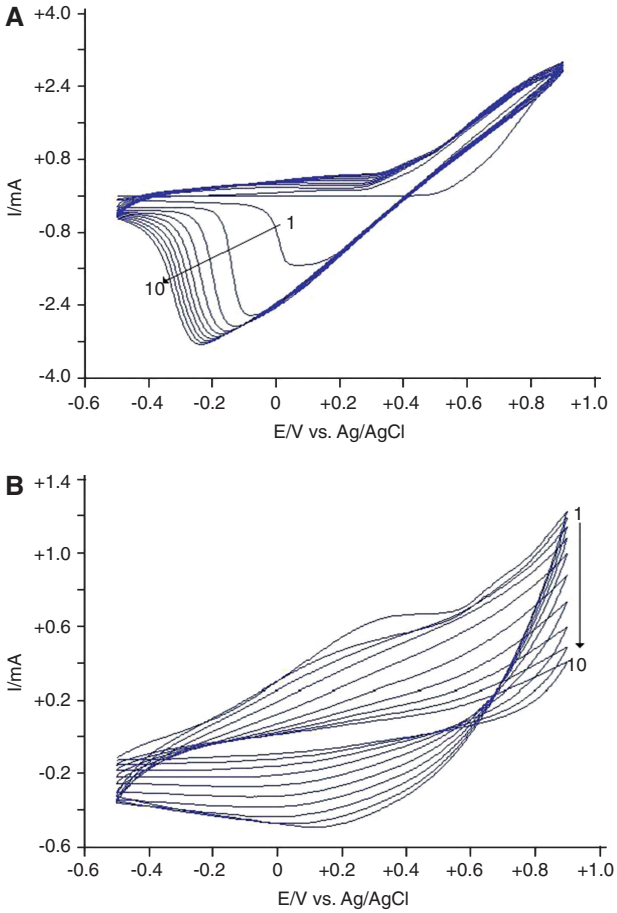

Figure 2 Cyclic voltammograms of 0.1 M Py solution in the presence of (A) 0.1 mol/L KI and (B) 0.1 mol/L KF. WE=VC, v=100 mV/s.

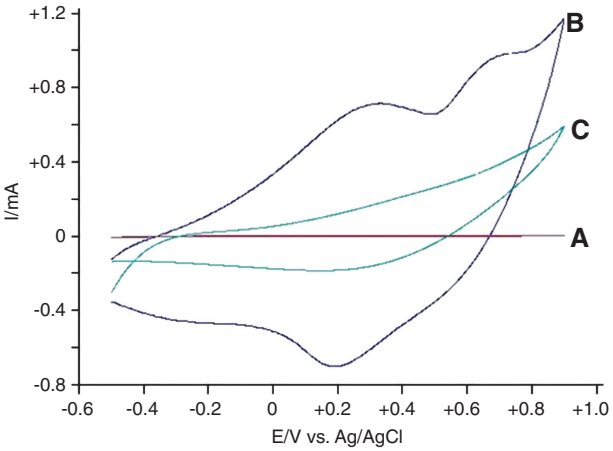

Figure 3 Electrochemical characterization of PPy films formed by cyclic voltammetry in 0.1 M KF on a VC electrode: (A) VC:PPy-F, (B) VC:PPy-F:PPy-I, and (C) VC:PPy-F:PPy-I:PPy-F.

electrochemical oxidation of Py (i.e., formation of PPy) starts at ca. 0.5 V.

Figure 2B shows the voltammograms corresponding to the formation of PPy films in 0.1 mol/L KF. These reveal that the incorporation of the anion in the PPy matrix is rather scant, as judged by the very small peak currents observed (i.e., below ±1.3 mA). Contrary to the experiments in KI, the anodic currents in KF decrease with the number of cycles, which is consistent with earlier reports (45) and is attributed to the oxidation of the monomer immediately followed by oxidation of the PPy adsorbed on the electrode surface. This leads to a current decrease that continues during each subsequent cycle corresponding to the oxidation of species between the bulk of the solution and the substrate (which then becomes passivated). Strong electrostatic interactions of the fluoride ions with the charge carriers have been deduced from X-ray photoelectron spectroscopy spectra and are believed to hinder PPy conductivity (46). This outcome provides a method for the production of passivated PPy thin films upon demand (1, 9, 10).

Figure 3 shows the electrochemical behavior of a composite sandwich-type film. A featureless curve (A) shows the voltammogram of the VC electrode in 0.1 mol/L KF. No redox signals appear here. The voltammogram (B) indicates the electrochemical formation of a PPy-F film in 0.1 mol/L KI solution. The area under the curve allows estimation of the amount of material formed. The voltammogram (C) shows the characterization of a second layer of PPy-F:PPy-I synthesized in a solution of KF and Py. Further deposition on the substrate previously modified by PPy-I yields a lower current and a smaller area under the curve, indicating that this second layer modifies the features of the previously formed deposit. In terms of conductivity, this result points at a passivation of the electrode surface (Figure 2B). Application of a second polymer layer doped with a different anion induces changes in the voltammogram, which are likely related to changes in the morphological and structural properties of the final PPy layer.

An alternative method for the production of conducting polymers involves the application of a constant potential with simultaneous monitoring of the current associated with the film formation process. Figure 4 shows the current vs. time curve for the first 60 s of PPy film formation on an Au (111) electrode in (A) 0.1 mol/L KI and (B) 0.1 mol/L KF.

It is obvious that different anions generate different electrochemical responses (39, 47). Many authors consider that this has a direct impact on the morphology and structure of the polymer films, as will be discussed further. Chainet et al. (48) investigated changes in film morphology and conductivity using different anions such as perchlorate, carbonate and trifluoromethanesulfonate. Their

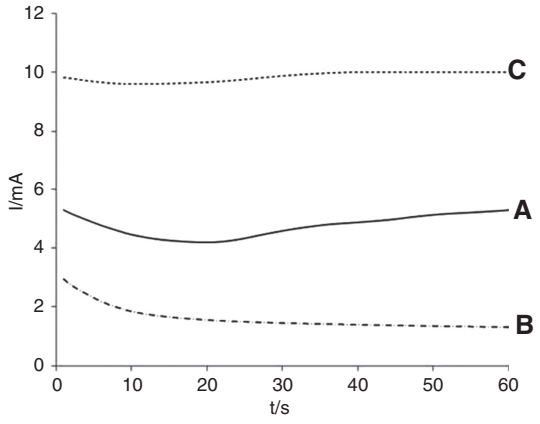

Figure 4 Electropolymerization of PPy films at a constant potential (i.e., +0.90 V vs. Ag/AgCl) on an Au (111) electrode in the presence of different anions: (A) Au:PPy-I, (B) Au:PPy-I:PPy-F, and (C) Au:PPy-I:PPy-F:PPy-I.

results show that film activity is not limited by surface variations but by the size of the counterion, which causes a significant effect on the micrometer-scale morphology via changes in the polymer electronic state. These changes are related to the ability to form either a conductive or a passive film, and they occur regardless of the technique employed for the formation of the polymeric material, the nature of the working electrode, and the sequence of steps to form a sandwich composite.

3.2 Morphological characterization of PPy films on Au (111)

The following study shows different arrangements (structures) that can be obtained by using different dopants (i.e., I^- or F^-) and by generating a composite sandwich-type deposit. In order to facilitate the monitoring of changes in the polymer film morphology, the perfectly ordered Au (111) electrode was used as a WE. Honbo et al. (49) showed that the uptake of Br^- or I^- species on Au (111) produces minor changes in the polymer properties. Other authors reached the same conclusion (50, 51).

3.3 Sandwich composite [Au:PPy-F:PPy-I:PPy-F]

Figures 5 and 6 show SEM micrographs obtained for the PPy film generated either by cyclic voltammetry using 10 polymerization cycles (from -0.5 to +0.9 V vs. Ag/AgCl) (Figure 5) or by the application of a constant potential (+0.90 V vs. Ag/AgCl) for 300 s with different anion dopants (Figure 6).

These results show that the electrode surface is modified by a polymer layer in both cases (i.e., using I^- or F^- as dopants). This alteration coincides with the results obtained in the electrochemical study (Figure 2), in which a passive film was obtained. In addition, this SEM monitoring also shows that the film is undergoing degradation and rearrangements of surface material. In agreement with this finding, Ratautaite et al. (52) have recently demonstrated that the application of high anodic potentials and repeated cycling during the electropolymerization of Py on Au electrodes may render electrochemical repulsion phenomena that facilitate PPy modulation for biomedical applications in scaffold design as well as the possible development of semipermeable membranes for water treatment purposes.

Figure 6 shows the PPy film formed at constant potential. The micrograph in Figure 6A shows the electrode surface covered by a PPy-F film with a typical layered structure, in sharp contrast with the morphology of the deposit obtained by cyclic voltammetry (Figure 5A). Further modification of the initial layer by PPy-I causes the rearrangement of the polymer surface into cluster or spherical microparticles (see Figure 6B). The average size of the individual microfeatures is between 0.6 and 1 µm, and they are connected in the form of a three-dimensional network. Such type of arrangement coincides with previous observations by Cruz et al. (53). Upon additional modification of the polymer surface in 0.1 mol/L Py and 0.1 mol/L KF, the microspheres open up and the film morphology changes significantly. The newly obtained features are referred to as cauliflower type by some authors (54).

3.4 Sandwich composite type [Au:PPy-I:PPy-F:PPy-I]

Figures 7 and 8 show SEM micrographs of films produced on Au (111) with the design described above and using different techniques: (A) cyclic voltammetry using 10 polymerization cycles in the potential range of -0.5 to +0.9 V vs. Ag/AgCl (Figure 7), or (B) applying a constant potential of +0.90 V vs. Ag/AgCl for 300 s (Figure 8).

Figure 7A shows a PPy film doped with KI on Au (111). The resulting morphology is substantially different from that of the first layer in the system doped with KF (Figure 5A). Microstructures are now observed in linear and circular forms on the surface in agreement with those obtained under different pH and anion dopant conditions (55–57). Some of these features are related to the grain morphology of the Au electrode. As noticed before, polymerization favors the edges of the grains.

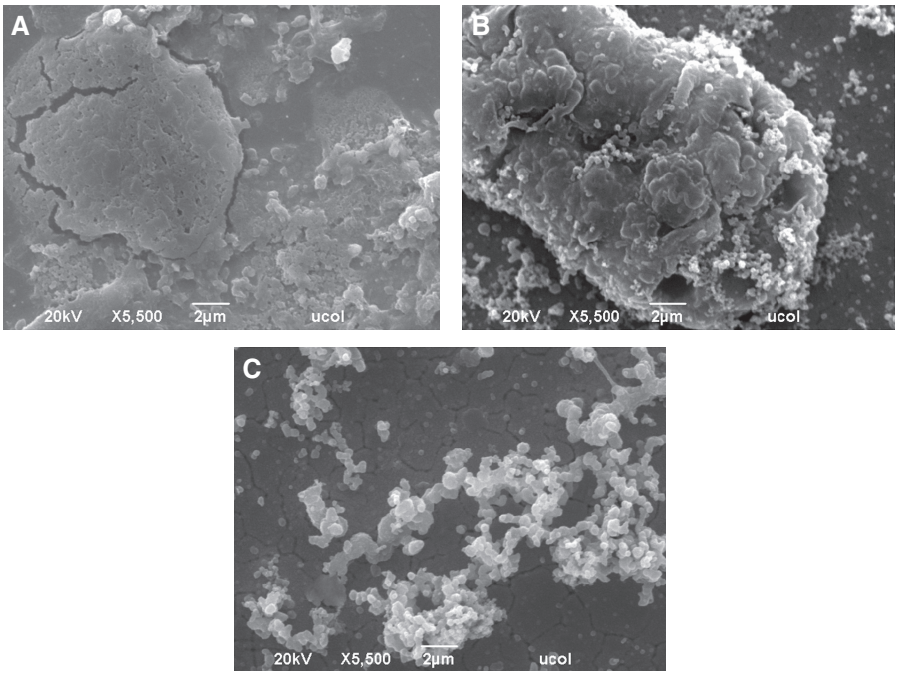

Figure 5 Typical SEM micrographs of PPy films produced by cyclic voltammetry in a potential range of -0.5 to +0.9 V vs. Ag/AgCl during 10 cycles, *v*=100 mV/s, on an Au (111) electrode: (A) Au:PPy-F, (B) Au:PPy-F:PPy-I, and (C) Au:PPy-F:PPy-I:PPy-F.

Figure 7B shows the same surface after applying a second polymeric layer (PPy-F). PPy film rearrangement takes place once more; the formation of semicircular tubes adds a new feature. Figure 7C evidently shows the growth of additional PPy-I layers in the form of semicircular structures. At the onset of the process, the polymer film morphologies are very similar but the new material (PPy-I) introduces significant modifications.

Variation of the polymerization technique (i.e., under constant potential) yields a completely different

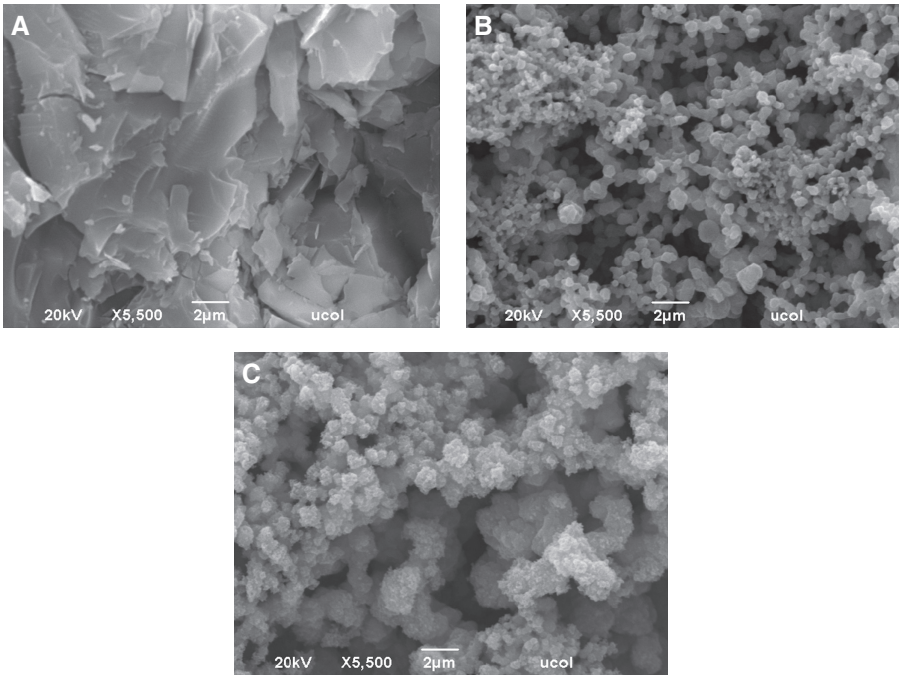

Figure 6 SEM micrographs of PPy films formed at a constant potential (+0.9 V vs. Ag/AgCl), *t*=300 s, in an aqueous medium and using the Au (111) working electrode: (A) Au:PPy-F, (B) Au:PPy-F:PPy-I, and (C) Au:PPy-F:PPy-I:PPy-F.

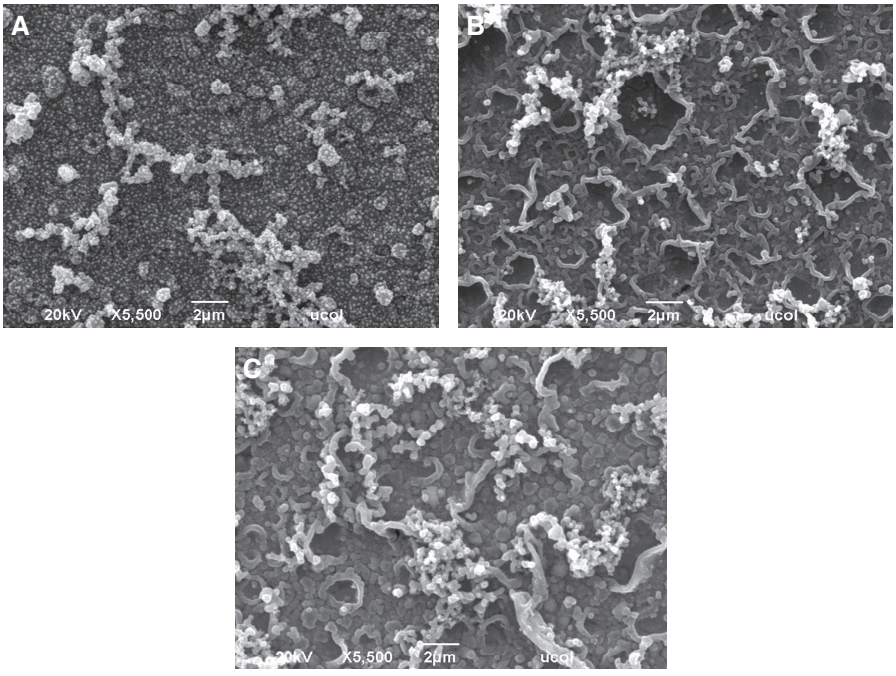

Figure 7 SEM micrographs of PPy films formed by cyclic voltammetry in a potential range of -0.5 to +0.9 V vs. Ag/AgCl during 10 cycles, *v*=100 mV/s, in an aqueous medium and using Au (111) as the working electrode: (A) Au:PPy-I, (B) Au:PPy-I:PPy-F, and (C) Au:PPy-I:PPy-F:PPy-I.

morphology. Figure 8A shows a polymer that evenly coats the surface of the Au (111) substrate, whereas nearly semicircular structures were obtained previously (Figure 6B).

Figure 8B shows changes that occur upon the application of a second layer of PPy doped with F^-, i.e., a degradation/surface modification process. Ring formation, which has been observed earlier due either to direct electrochemical oxidation (58) or to the presence of Cl^- in the medium (59), becomes evident. It has been suggested that these PPy films may suffer degradation under oxidative stress, as supported by SEM images in which polymer degradation zones are observed. Figure 8B also supports this view (see the circular features and the dark-colored zones) (59).

Figure 8C shows a verge on this area (next to the newly formed ring). This indicates that the dopant anion (i.e., F^-) is accelerating the overoxidation of the material formed, which results in a decrease in the area under the electrochemical response curve and an apparent material degradation in the SEM images. Figure 8C also shows the formation of a PPy-I layer on top of the earlier material shown in Figure 8B. As the PPy deposition tends to coat the doughnut-shaped structures, growth is preferred in this area and a microcontainer is formed as time evolves. This provides an alternative design method. Several authors have prepared different types of microcontainers in the form of bubbles using PPy polymerized onto H_2 bubbles to apply them in sensors, catalysts, microreactors, and drug-eluting systems (60). Other authors have built microcontainers by growing PPy in different shapes (e.g., cups, cans, and bowls) through the application of Py oxidation in aqueous media using a solution of β-naphthalenesulfonic acid (61). The results obtained in the present investigation are consistent with those reported by these authors since the formation of such structures is obtained by applying an oxidation potential to the system, particularly if the overoxidation of the previous layer favors the formation of key structures as this process promotes the formation of rings in which the microcontainer shape is obtained. Caballero et al. (62) have recently achieved PPy ring formation by using an elegant electropolymerization-submerged microcontact printing technique. Gao et al. (63) designed microcontainers using self-assembled layers formed with PPy and different materials with defined structures formed on a conductive glass substrate covered by indium tin oxide (ITO). Interestingly, the Py monomer concentration modifies the final surface characteristics.

Elucidation of the nucleation and growth mechanism is possible only in the early stages of polymer formation through a current transient analysis. For example, in the presence of $LiClO_4$ an instantaneous nucleation with two-dimensional growth was found, together with a three-dimensional progressive nucleation with diffusion-controlled growth (64). Irregular morphologies have been observed by atomic force microscopy (AFM) or SEM

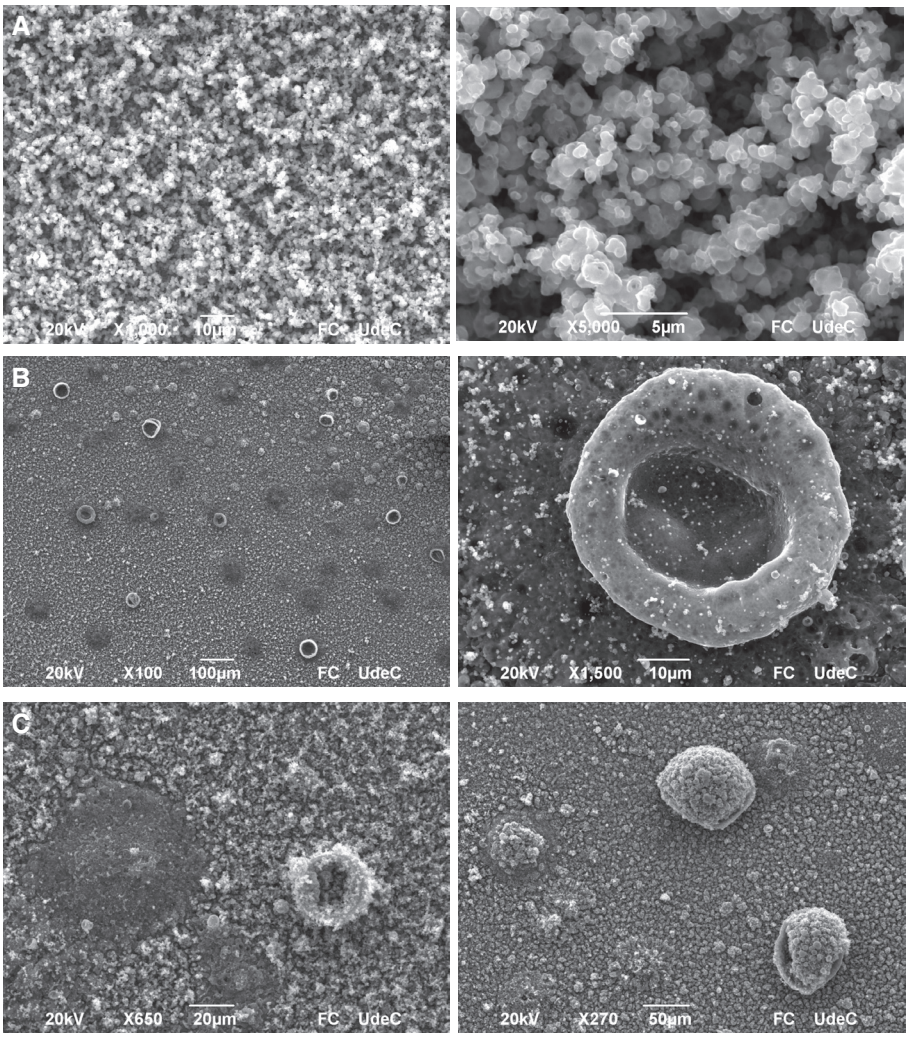

Figure 8 SEM micrographs of PPy films formed at constant potential (+0.9 V vs. Ag/AgCl), *t*=300 s, on an Au (111) electrode: (A) Au:PPy-I, (B) Au:PPy-I:PPy-F, and (C) Au:PPy-I:PPy-F:PPy-I. Note the different amplifications in the left micrographs vs. those in the right.

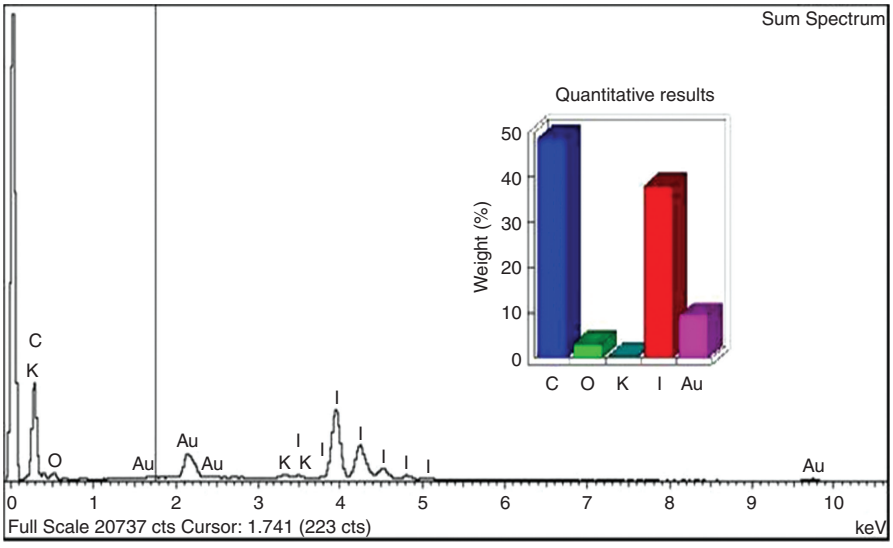

Figure 9 Quantitative analysis of the Au (111) surface: PPy-I:PPy-F:PPy-I.

that may be indicative of progressive processes (65–67). However, great care must be exercised in the drawing of conclusions when AFM images are observed only once and in a specific section. It would be considerably more reliable to follow the target process *in situ* and in real time. Unfortunately, this is not possible due to the rapid polymerization kinetics involved.

Nonetheless, the unique PPy film morphology grown with F^- as dopant is clearly demonstrated in the present study. The foremost features involve uniformly shaped small nodules (40–80 nm) and a regular film surface tracking the flat substrate, possibly indicating instantaneous nucleation and growth.

The different morphologies between layers grown in solutions containing different dopants represent an important factor in the final properties of the sandwiched films, which display a remarkable capacity for microcontainer formation.

As described above, the type of microstructures formed in the present study can, in principle, find alternative applications as substrates for drug delivery. Since PPy is biocompatible and has the ability to degrade when needed, this would allow drug release by changing key conditions in the medium.

The results obtained herein indicate that the presence of different anions changes the morphological features of the formed films. Figure 9 shows the results obtained by EDS (Sun Spectrum), where the quantitative surface analysis reveals the presence of carbon forming the main structure of PPy; oxygen attributed to a possible overoxidation of the material by its presence in the medium during layer formation with KF+Py (under an anodic applied potential); gold, which corresponds to the substrate used; and iodine as dopant anion within the structure of the polymeric material. The absence of an F signal indicates that this material is not incorporated into the material to a significant extent. The analysis of the area in Figure 8B shows that the ring formed contains mostly carbon.

In summary, PPy films with controllable geometries can be obtained by modulating selected parameters during their electrosynthesis. Several properties are related to the nature of the anion (dopant) used during film preparation. PPy features, including ring and microcontainer structures, can be generated by pyrrole electropolymerization in aqueous solutions with different dopant anions (i.e., I^- or F^-). The overoxidation of PPy in the presence of the F^- anion modifies the morphological characteristics and produces the formation of different shapes and sizes on the surface.

Acknowledgments: We acknowledge funding through CONACyT-Mexico (project nos. CB-2006-1-61242 and CB-2012-177480) and ICyTDF-Mexico (project no. 12411497), and the University of Colima for facilitating the SEM-EDS equipment.

Received August 17, 2013; accepted October 16, 2013

References

1. Ponce de Leon C, Campbell SA, Smith JR, Walsh FC. Conducting polymer coatings in electrochemical technology. Part II. Application areas. Trans Inst Met Finish. 2008;86(1):34–40.
2. Cheng Y, Liu M, Zhang Y, Niu Y, Huang F, Ka J, Yip H, Tian Y, Jen A. Synthesis and characterization of hole-transporting materials using styrene as an efficient thermally crosslinkable group for light-emitting devices. Chem Mater. 2008;20(2):413–22.
3. Hu L, Gruner G, Li D, Kaner R, Cech J. Patternable transparent carbon nanotube films for electrochromic devices. J Appl Phys. 2007;101(1):16102–5.
4. Aydemir K, Tarkuc S, Durmus A, Gunbas G, Toppare L. Synthesis, characterization and electrochromic properties of a near infrared active conductive polymer of 1,4-di(selenophen-2-yl)-benzene. Polymer. 2008;49(8):2029–32.
5. Padilla J, Seshadri V, Otero TF, Sotzing G. Electrochemical study of dual conjugated polymer electrochromic devices. J Electroanal Chem. 2007;609(2):75–84.
6. Ateh D, Waterworth A, Walker D, Brown B, Navsaria H, Vadgama P. Impedimetric sensing of cells on polypyrrole-based conducting polymers. J Biomed Mater Res A. 2007;83(2):391–400.
7. Grgur B, Gvozdenović M, Stevanović J, Jugović B, Marinović V. Polypyrrole as possible electrode material for the aqueous-based rechargeable zinc batteries. Electrochim Acta. 2008;53(14):4627–32.
8. Nakahara K, Iriyama J, Iwasa S, Suguro M, Satoh M, Cairns E. High-rate capable organic radical cathodes for lithium rechargeable batteries. J Power Sources. 2007;165(2):870–3.
9. Rammelt U, Nguyen PT, Plieth W. Corrosion protection by ultrathin films of conducting polymers. Electrochim Acta. 2003;48(9):1257–62.
10. Redondo MI, Breslin CB. Polypyrrole electrodeposited on copper from an aqueous phosphate solution: Corrosion protection properties. Corros Sci. 2007;49(4):1765–76.
11. Ahuja T, Mir I, Kumar D, Rajesh C. Biomolecular immobilization on conducting polymers for biosensing applications. Biomaterials. 2007;28(5):791–805.
12. Carquigny S, Segut O, Lakard B, Lallemand F, Fievet P. Effect of electrolyte solvent on the morphology of polypyrrole films: application to the use of polypyrrole in pH sensors. Synth Met. 2008;158(11):453–61.

13. Radhakrishnan S, Paul S. Conducting polypyrrole modified with ferrocene for applications in carbon monoxide sensors. Sens Actuators B. 2007;125(1):60–5.
14. Vernitskaya TV, Efimov ON. Polypyrrole: a conducting polymer: its synthesis, properties and applications. Russ Chem Rev. 1997;66(5):443–57.
15. Schoch K,Saunders H. Conducting polymers. IEEE Spectrum. 1992;29(6):52–5.
16. Fredrickson G. Theoretical profits. Nat Mat. 2008;7(4):261–3.
17. Greef T, Meijer E. Supramolecular polymers. Nature. 2008;453(7192):171–3.
18. Heinze J, Frontana-Uribe B, Ludwigs S. Electrochemistry of conducting polymers persistent models and new concepts. Chem Rev. 2010;110(8):4724–71.
19. Qi Z, Pickup P. Size control of polypyrrole particles. Chem Mater. 1997;9(12):2934–9.
20. Sadki S, Schottland P, Brodie N, Sabouraud G. The mechanisms of pyrrole electropolymerization. Chem Soc Rev. 2000;29: 283–93.
21. Otero TF, Sansiñena JM. Influence of synthesis conditions on polypyrrole-poly(styrenesulphonate) composite electroactivity. J Electroanal Chem. 1996;412:109–16.
22. Ehsani A, Mahjani MG, Jafarian M, Naeemy A. Electrosynthesis of polypyrrole composite film and electrocatalytic oxidation of ethanol. Electrochim Acta. 2012;71:128–33.
23. Ge D, Tian X, Qi R, Huang S, Mu J, Hong S, Ye S, Zhang X, Li D, Shi W. A polypyrrole-based microchip for controlled drug release. Electrochim Acta. 2009;55(1):271–5.
24. Svirskis D, Travas-Sejdic J, Rodgers A, Garg S. Electrochemically controlled drug delivery based on intrinsically conducting polymers. J Control Rel. 2010;146(1):6–15.
25. Ebrahimzadeh H, Mehdinia A, Kamarei F. A sensitive method for the determination of methadone in biological samples using nano-structured α-carboxy polypyrrole as a sorbent of SPME. Chromatographia. 2012;75(3–4):149–55.
26. Alvarez-Romero G, Ramirez-Silva M, Galan-Vidal C, Paez-Hernandez M, Romero-Romo M. Development of a chloride ion-selective solid state sensor based on doped polypyrrole-graphite-epoxy composite. Electroanalysis. 2010; 22(14):1650–4.
27. Ebrahimzadeh H, Mehdinia A, Yamini Y, Kasraee S, Gholizade A. Analysis of mono-nitrotoluenes in water samples by using nano-structured polypyrrole as a sorbent of solid-phase microextraction. Int J Environ Anal Chem. 2010;90(13):963–75.
28. Patois T, Lakard B, Monney S, Roizard X, Fievet P. Characterization of the surface properties of polypyrrole films. Influence of the electrodeposition parameters. Synth Met. 2011;161(21–22):2498–505.
29. Varade V, Honnavar GV, Anjaneyulu P, Ramesh KP, Menon R. Probing disorder and transport properties in polypyrrole thin-film devices by impedance and Raman spectroscopy. J Phys. D: Appl Phys. 2013;46(36):365306.
30. Shimidzu T, Ohtani A, Honda K. Dual-mode behavior in doping-undoping of polypyrrole with alkanesulfonate. Bull Chem Soc Jap. 1988;61(8):2885–90.
31. Gupta S. Template-free synthesis of conducting-polymer polypyrrole micro/nanostructures using electrochemistry. Appl Phys Lett. 2006;88(6):063108-1–3.
32. Adhikaria A, Radhakrishnanb S, Patil R. Influence of dopant ions on properties of conducting polypyrrole and its electrocatalytic activity towards methanol oxidation. Synth Met. 2009; 159(15–16):1682–8.
33. Stankovic R, Pavlovic O, Vojnovic M, Jovanovic S. The effects of preparation conditions on the properties of electro-chemically synthesized thick films of polypyrrole. Eur Polym J. 1994;30(3):385–93.
34. Silk T, Hong Q, Tamm J, Compton RG. AFM studies of polypyrrole film surface morphology – I. The influence of film thickness and dopant nature. Synth Met. 1998;93(1):59–64.
35. Tang Y, Mu S, Chen H. Electrochemical synthesis of polypyrrole for the immobilization of galactose oxidase. Synth Met. 1998;92(2):173–8.
36. Curtin L, Komplin G, Pietro W. Diffusive anion exchange in polypyrrole films. J Phys Chem. 1988;92(1):12–3.
37. Silk T, Hong Q, Tamm J, Compton RG. AFM studies of polypyrrole film surface morphology. II. Roughness characterization by the fractal dimension analysis. Synth Met. 1998;93(1):65–71.
38. Suarez MF, Compton RG. In situ force microscopy study of polypyrrole synthesis and the volume changes induced by oxidation and reduction of the polymer. J Electroanal Chem. 1999;462:211–21.
39. Mahjani MG, Ehsani A, Jafarian M. Electrochemical study on the semiconductor properties and fractal dimension of polyor-thoaminophenol modified graphite electrode in contact with different aqueous electrolytes. Synth Met. 2010;160:1252–8.
40. Páramo-García U, Ibanez JG, Batina N. Electrochemical modulation of the thickness of polypyrrole films by using different anionic dopants. Int J Electrochem Sci. 2011;6: 5172–88.
41. Alatorre MA, Gutierrez S, Paramo U, Ibanez JG. Reduction of hexavalent chromium by polypyrrole deposited on different carbon substrates. J Appl Electrochem. 1998;28(5):551–7.
42. Lindfors T, Bobacka J, Ivaska A. Electrosynthesis of polypyrrole in iodide solution — film growth, redox behavior and potentiometric response. Anal Chim Acta. 1997;355(2–3): 217–25.
43. Bull R, Fan F, Bard A. Polymer films on electrodes: 7. Electro-chemical behavior at polypyrrole-coated platinum and tantalum electrodes. J Electrochem Soc. 1982;129(5):1009–15.
44. Heinze J, Rasche A, Pagels M, Geschke B. On the origin of the so-called nucleation loop during electropolymerization of conducting polymers. J Phys Chem. B. 2007;111(5):989–97.
45. Schneider O, Schwitzgebel G. The mechanism of electrode passivation during the electrodeposition of polypyrrole from aqueous solutions containing fluoride anions. Synth Met. 1998;93(3):219–25.
46. Yfantis A, Appel G, Schmeisser D, Yfantis D. Polypyrrole doped with fluoro-metal complexes: thermal stability and structural properties. Synth Met. 1999;106(3):187–95.
47. Elmansouri A, Outzourhit A, Lachkarb A, Hadik N, Abouelaoualim A, Achour ME, Oueriagli A, Ameziane EL. Influence of the counter ion on the properties of poly(o-toluidine) thin films and their Schottky diodes. Synth Met. 2009;159(3–4):292–7.
48. Chainet E, Billon M. In situ STM study of the counterion effect on the doping stages of polypyrrole films. Synth Met. 1999;99(1):21–6.
49. Honbo H, Sugawara S, Itaya K. Detailed in situ scanning tunneling microscopy of single crystal planes of gold(111) in aqueous solutions. Anal Chem. 1990;62(5):2424–9.

50. Li M, Cui Y, Gao M, Luo J, Ren B, Tian Z. Clean substrates prepared by chemical adsorption of iodide followed by electrochemical oxidation for surface-enhanced Raman spectroscopic study of cell membrane. Anal Chem. 2008;80(13):5118–25.
51. Tao N, Lindsay S. In-situ scanning tunneling microscopy of iodine and bromine adsorption on Au(111) under potential control. J Phys Chem. 1992;96(3):5213–7.
52. Ratautaite V, Ramanaviciene A, Oztekin Y, Voronovic J, Balevicius Z, Mikoliunaite L, Ramanavicius A. Electrochemical stability and repulsion of polypyrrole film. Coll Surf. A. 2013;418:16–21.
53. Cruz G, Olayo M, López O, Gómez L, Morales J, Olayo Y. Nanospherical particles of polypyrrole synthesized and doped by plasma. Polymer. 2010;51(19):4314–9.
54. Kaynak A, Yang C, Lim Y, Koizani A. Electrochemical fabrication and modelling of mechanical behavior of a tri-layer polymer actuator. Mat Chem Phys. 2011;125(1–2):113–7.
55. Wei M, Dai T, Lu Y. Controlled fabrication of nanostructured polypyrrole on ion association template: Tubes, rods and networks. Synth Met. 160(9–10):849–54.
56. Schulz B, Orgzall I, Díez I, Dietzel B, Tauer K. Template mediated formation of shaped polypyrrole particles. Coll Surf. A: Physicochem Eng Aspects. 2010;354(1–3):368–76.
57. Mao H, Li Y, Liu X, Zhang W, Wang C, Al-Deyab S. The application of novel spindle-like polypyrrole hollow nanocapsules containing Pt nanoparticles in electrocatalysis oxidation of nicotinamide adenine dinucleotide (NADH). J Coll Interf Sci. 2011;356(2):757–62.
58. Fujikawa K, Jung H, Park J, Kim J, Lee H, Kawai T. AFM imaging of nanostructure polypyrrole doughnuts shapes fabricated by direct electrochemical oxidation. Electrochem Commun. 2004;6(5):461–4.
59. Ibanez JG, Alatorre-Ordaz MA, Gutierrez-Granados S, Batina N. Nanoscale degradation of polypyrrole films under oxidative stress: an atomic force microscopy study and review. Polym Degrad Stab. 2008;93(4):827–37.
60. Kim J, Seol S, Je J, Hwu Y, Margaritondo G. The microcontainer shape in electropolymerization on bubbles. Appl Phys Lett. 2009;94(3):034103-1–3.
61. Qu L, Shi G, Chen F, Zhang J. Electrochemical growth of polypyrrole microcontainers. Macromolecules. 2003;36(4):1063–7.
62. Caballero D, Fumagalli L, Teixidor F, Samitier J, Errachid A. Directing polypyrrole growth by chemical micropatterns: a study of high-throughput well-ordered arrays of conductive 3D microrings. Sensor Actuat. B: Chem. 2013;177:1003–9.
63. Gao Y, Zhao L, Bai H, Chen Q, Shi G. Electrosynthesis of small polypyrrole microcontainers. J Electroanal Chem. 2006;597(1):13–8.
64. Arteaga GC, Del Valle MA, Antilén M, Romero M, Ramos A, Hernández L, Arévalo MC, Pastor E, Louarn G. Nucleation and growth mechanism of electro-synthesized poly(pyrrole) on steel. Int J Electrochem Sci. 2013;8(3):4120–30.
65. Páramo-García U, Ibañez JG, Batina N. AFM analysis of polypyrrole films synthesized in the presence of selected doping agents. Int J Electrochem Sci. 2013;8:2656–69.
66. Chmielewski M, Grzeszczuk M, Kalenik J, Kepas-Suwara A. Evaluation of the potential dependence of 2D-3D growth rates and structures of polypyrrole films in aqueous solutions of hexafluorates. J Electroanal Chem. 2010;647(2):169–80.
67. Licona-Sánchez T, Álvarez-Romero G, Mendoza-Huizar L, Galan-Vidal CA, Palomar-Pardavé M, Romero-Romo M, Herrera-Hernández H, Uruchurtu J, Juárez-García J. Nucleation and growth kinetics of electrodeposited sulfate-doped polypyrrole: determination of the diffusion coefficient of SO_4^{2-} in the polymeric membrane. J Phys Chem. B. 2010;114(30):9737–43.